

## EFFICIENCY OF COMBINED Fe AND Pb RADIATION SHIELD OF TRANSPORT CASKS FOR SNF TRANSPORTATION

V.G. Rudychev<sup>1</sup>, M.O. Azarenkov<sup>2,1</sup>, I.O. Girka<sup>1</sup>, Y.V. Rudychev<sup>2,1</sup>

<sup>1</sup>V.N. Karazin Kharkiv National University, Kharkiv, Ukraine;

<sup>2</sup>National Science Center "Kharkov Institute of Physics and Technology", Kharkiv, Ukraine

E-mail: vrudychev@karazin.ua

The possibility of increasing the efficiency of combined iron and lead shielding of transport containers (TC) for SNF transportation by railroad is studied. Models for the transport of SNF  $\gamma$ -quanta are developed, that make it possible to determine the dose rates behind thick shields using the Monte Carlo method. It is shown that for layers of the same mass thickness: the layer of Fe with the thickness of 15 cm, and the layer of Pb with the thickness of 10.4 cm which is equivalent to 15 cm of iron, placement of Fe in the first layer, and Pb in the second layer provides increase of attenuation of the gamma flux by more than 2 times as compared with the reverse order. The attenuation of SNF neutrons by Fe and Pb shields is studied. The gamma flux from SNF can be decreased by  $\sim 1.5$  times by placement of the most of Fe to the first layer without changing the weight of both layers, in the HI-STAR190UA TC.

### INTRODUCTION

A significant part of the transportation of spent nuclear fuel (SNF) is carried out by railroad in transport casks (TC) [1]. TC is a complex technical structure of a cylindrical shape weighting  $\sim 100 \dots 150$  t. SNF is placed in a sealed cylindrical container with a diameter of up to 2 m surrounded by radiation shielding from gamma rays and neutrons. Gamma radiation shield is a thick-walled layered hollow cylinder made of steel or cast iron up to 30 cm thick [2]. The neutron shield, which surrounds gamma shield, is made of light materials: rubber, plastic, etc. The main weight of the radiation shield is formed by the gamma shield. The flux of  $\gamma$ -quanta and neutrons of the transported fuel is determined by the level of burnup and the SNF cooling time in the NPP spent fuel pools. The effectiveness of radiation shield determines the amount of SNF transported in the TC in the form of spent fuel assemblies (SFAs). Up to 32 SFAs with a burnup of  $\leq 45$  (MW day)/kg and a cooling time of more than 7 years are transported in such casks. The number of permitted for transportation SFAs decreases with increase in the level of burnup and decrease in cooling time: it can be even smaller than twenty. TCs with combined shield from lead and steel were developed for transportation of 26...31 SFAs with the burnup of 45...55 MW day/kg and the cooling time of 5...7 years. The thickness of gamma radiation shield of the NAC-STC container (26 SFAs) developed by NAC International is 10.5 cm for Fe and 9.4 cm for Pb [2]. For the HI-STAR190UA cask (31 SFAs), developed by HOLTEK for the transportation of SNF from Ukrainian NPPs for dry storage at the Central Nuclear Fuel Storage Facility, the thicknesses of gamma shield are 14.4 cm for Fe and 14.1 cm for Pb [3]. It should be noted, that thermal calculations for such kind systems were carried out e.g. in [4, 5].

The purpose of the present paper is to study the influence of the placement order and thickness of Fe and Pb layers on the gamma and neutrons radiation transport from long-lived SNF isotopes through shielding of large mass thickness.

### 1. CALCULATION METHOD

Taking into account the dimensions of the TCs, the passage of gamma and neutrons radiation through the thick-walled shield, equivalent to the shield of the TC, is simulated by the Monte Carlo method. The radiation source was simulated in the PHITS [6] as a cylinder of 1.8 m in diameter and 3.5 m long filled with SNF, surrounded by layered cylindrical shields. The elemental composition of the fuel emission zone, which is planned to be transported in the TCs to the storage by the dry method, was modeled by homogeneous SNF with a density of  $3.5 \text{ g/cm}^3$  containing  $^{238}\text{U}$  52.3%,  $^{40}\text{Zr}$  25.8%,  $^{26}\text{Fe}$  14.6%,  $^{16}\text{O}$  7.3% [8]. It is shown in [7] that the flux of  $\gamma$ -quanta on the surface of the source is determined by the near-surface layer of SNF. As the initial characteristics of  $\gamma$ -quanta, the energy and angular distributions of  $\gamma$ -radiation from a layer of homogenized SNF  $\approx 10$  cm thick were used. The data obtained as simulation result from a source in the form of a cylindrical layer of homogenized SNF  $\approx 10$  cm thick is used as initial characteristics of  $\gamma$ -radiation angular distributions. In contrast to the gamma radiation shield, the radiation of neutrons on the surface of the shield is determined by the entire volume of SNF. Fig. 1 shows the change in the photon flux simulated by PHITS during the gamma radiation passage of the  $^{60}\text{Co}$  isotope through the four-layer shield of Fe and Pb.

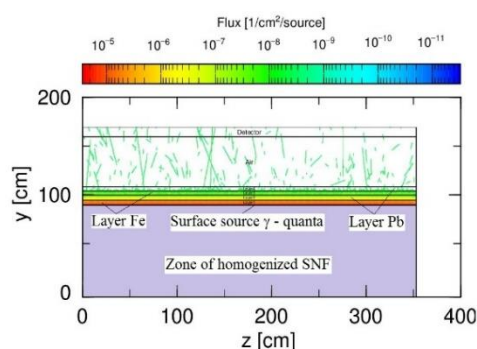


Fig. 1. Photon flux passing through four-layer shield of Fe and Pb

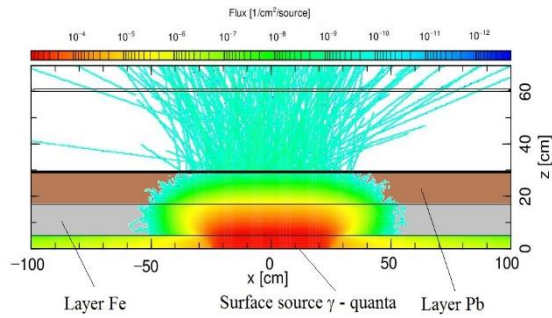


Fig. 2. Photon flux passing through two-layer shield of Fe and Pb

The study of the shielding parameters effect on the characteristics of transmitted photons requires a significant amount of time for Monte Carlo calculations due to the large dimensions of both the source (the height is 3.5 m and the diameter is 1.8 m) and shields. To speed up the calculations, which make it possible to study the influence of the thicknesses of Fe and Pb layers on the characteristics of the shielded radiation, a simulation model of a flat layered shield with a flat surface source of  $\gamma$ -quanta was produced using PHITS. The radiation shield is modeled as a set of disks of different materials of different thicknesses with a diameter of 2 m and a surface source of  $\gamma$ -quanta in the form of a disk with a diameter of 0.5 m or more. The energy and angular distributions of  $\gamma$ -radiation used in the surface disk source are similar to those used in the

cylindrical model. Note that the results of calculations of the change in  $\gamma$ -radiation when passing through shields of the same thickness in the models of cylindrical and disk surface sources differ by 1...2%. The change in the photon flux simulated by PHITS for the passage of radiation  $\gamma$ -quanta of the  $^{60}\text{Co}$  isotope through a two-layer shield of Fe and Pb is shown in Fig. 2.

The speed of calculations in the model of a disk surface source is 3–5 times higher than in the model of a cylindrical source, which provides a statistical error of less than 5% for large shield thicknesses. Cylindrical and disk models make it possible to calculate the attenuation of radiation both for given energies of  $\gamma$ -quanta, and for  $\gamma$ -quanta of the SNF spectrum. External  $\gamma$ -TC radiation at a given burnup and SNF cooling time is determined by long-lived isotopes. When determining the transport of  $\gamma$ -quanta through shield for the main isotopes, it is possible to determine the effectiveness of SNF shield for a given burnup and storage time. At storage times of more than five years, the  $^{134}\text{Cs}$ ,  $^{137\text{m}}\text{Ba}$  ( $^{137}\text{Cs}$ ),  $^{154}\text{Eu}$ , and  $^{60}\text{Co}$  isotopes, whose half-life is longer than one year, make the maximum contribution to  $\gamma$ -radiation outside the TC [8]. Table 1 lists the main characteristics of these isotopes: half-lives  $T_{1/2} > 1$  year, energies of  $\gamma$ -quanta whose quantum yields are greater than 5% of the total yield  $Y_i$ .

Table 1

Characteristics of isotopes: half-lives  $T_{1/2} > 1$  year, energies of  $\gamma$ -quanta, and quantum yields which are larger than 5% of the total yield  $Y_i$

No	Isotope	$T_{1/2}$ , year	$E\gamma$ , MeV (yield/1Bq, > 5% total)	$Y_i$ , yield/1Bq, total ( $E\gamma > 0.2$ MeV)
1	$^{60}\text{Co}$	5.27	1.17 (0.999); 1.33 (0.9998)	2
2	$^{134}\text{Cs}$	2.06	0.57 (0.15); 0.60 (0.975); 0.8 (0.851)	2.224
3	$^{137\text{m}}\text{Ba}$ ( $^{137}\text{Cs}$ )	30	0.662 (0.9)	0.9
4	$^{154}\text{Eu}$	8.6	0.6 (0.061); 0.72 (0.2); 0.87 (0.115); 1.0 (0.28); 1.27 (0.355)	1.22

The spontaneous fission of  $^{244}\text{Cm}$ , the half-life of which is 18.1 years, is the main source of neutrons produced by SNF (about 97.4%) [9]. The neutron spectrum of spontaneous fission of actinides is similar to the spectrum of stimulated fission of  $^{235}\text{U}$  and is approximated by the relation [10]

$$N(E) = \frac{2\sqrt{E}}{\sqrt{\pi}\theta^3} \exp(-E/\theta), \quad (1)$$

where  $E$  is the energy, MeV, and  $\theta$  is the hardness parameter, equal to 1.33 MeV for  $^{244}\text{Cm}$ . The average energy of such neutrons is approximately 1.995 MeV.

## 2. CALCULATION RESULTS

The effectiveness of shields from layers of different thicknesses, as well as the order of their placement with keeping the shield weight, i.e. at a constant mass thickness of the shield in units of  $\text{g}/\text{cm}^2$  were investigated in [11]. The thickness of lead in the present paper is replaced by the equivalent Fe thickness:

$t_{\text{eq}}^{\text{Pb}} = t_{\text{Pb}} \cdot \rho_{\text{Pb}} / \rho_{\text{Fe}}$ . Here  $t_{\text{Pb}}$  is the thickness of Pb in cm,  $\rho_{\text{Fe}}$  and  $\rho_{\text{Pb}}$  are the mass densities of Fe and Pb. The thickness of the combined shield made from Fe and Pb, which is equivalent to the Fe thickness, is determined as  $t_{\text{eq}} = t_{\text{Fe}} + t_{\text{eq}}^{\text{Pb}}$ . The mass thicknesses of the radiation protection are  $\approx 189 \text{ g}/\text{cm}^2$  and  $\approx 273 \text{ g}/\text{cm}^2$ , and  $t_{\text{eq}} \approx 24 \text{ cm}$  and  $t_{\text{eq}} \approx 35 \text{ cm}$  for the NAC-STC TC and for the HI-STAR190UA TC, respectively. Table 2 shows the magnitudes of the Pb thicknesses in cm and corresponding Fe-equivalent thickness  $t_{\text{eq}}^{\text{Pb}}$  in cm.

Table 2

Values of the Pb thicknesses and the corresponding Fe equivalent thicknesses  $t_{\text{eq}}^{\text{Pb}}$  in cm

$t_{\text{Pb}}$ , cm	10.39	13.85	17.31	20.78	24.24
$t_{\text{eq}}^{\text{Pb}}$ , cm	15	20	25	30	35

To compare the effectiveness of attenuation of gamma-ray fluxes, the doses produced by  $\gamma$ -quanta of different energies behind shields made of Fe and Pb of different thicknesses are calculated. The dose rates

subject to the energy of  $\gamma$ -quanta for the energy range of 0.4...1.65 MeV after passing through shields made of Fe 20, 25, 30 cm thick and Pb with a thickness  $t_{pb}$  equivalent to Fe 20, 25, 30 cm, respectively are shown in Fig. 3 (see Table 1).

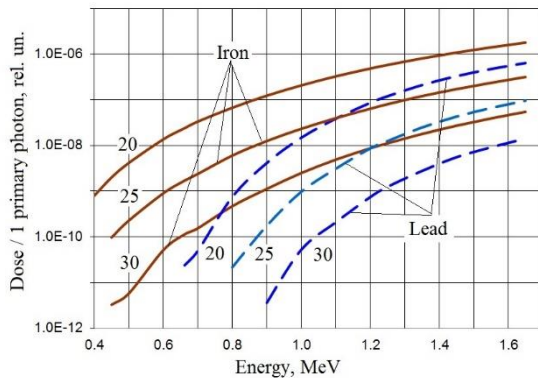


Fig. 3. The dose rates subject to the energy of  $\gamma$ -quanta for the energy range of 0.4...1.65 MeV after passing through various shields

The ratio  $D_{Pb}/D_{Fe}$ , which characterizes the effectiveness of shields made of Pb compared to Fe shield, is presented in Fig. 4. Here  $D_{Pb}$  is the dose rate after passing through the shield made of Pb, and  $D_{Fe}$  is the dose rate after passing through iron shield, respectively.

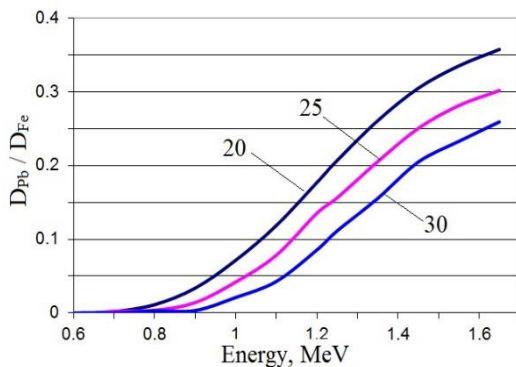


Fig. 4. The ratio  $D_{Pb}/D_{Fe}$ , which characterizes the effectiveness of shields made of Pb compared to Fe shield

It follows from the data shown in Fig. 4 that, for large shield thicknesses, the efficiency of lead shield is significantly higher than iron shield, especially for low energies of  $\gamma$ -quanta.

The shield efficiencies  $D_{Pb}/D_{Fe}$  subject to the equivalent Fe shield thickness for  $\gamma$ -quanta from isotopes  $^{60}\text{Co}$ ,  $^{134}\text{Cs}$ ,  $^{137}\text{Cs}$ ,  $^{154}\text{Eu}$  are presented in Fig. 5. It follows from the data presented in Fig. 5, that the efficiency of the Pb shield increases with an increase in its thickness due to the attenuation of the radiation of high-energy  $\gamma$ -quanta of  $^{60}\text{Co}$  and  $^{154}\text{Eu}$  isotopes. Average energies of  $\gamma$ -quanta are 1.25 and 1.0 MeV for  $^{60}\text{Co}$  and  $^{154}\text{Eu}$  isotopes, respectively, if  $E_\gamma$  is larger than 0.4 MeV. The efficiency of Pb shield for  $\gamma$ -quanta of the  $^{134}\text{Cs}$  isotope is practically independent of the shielding thickness, the average energy is  $E_{Cs4} \approx 0.7$  MeV. For the  $^{137}\text{Cs}$  isotope, whose emission gamma energy is  $E_{Cs7} = 0.662$  MeV, the efficiency of Pb shield is  $\sim 0.004$  at  $t_{eq} = 15$  cm, and  $\sim 0.001$  at  $t_{eq} = 20$  cm.

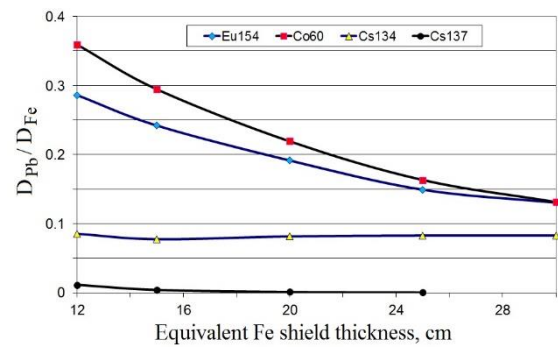


Fig. 5. Shield efficiencies  $D_{Pb}/D_{Fe}$  vs the equivalent Fe shield thickness

Features of the transformation of the spectrum of primary photons from the  $^{154}\text{Eu}$  isotope, which contains the photons with energies both smaller and larger than 1 MeV, during their passage through the Fe and Pb shields are shown in Fig. 6. Absorption of high-energy photons, whose energy is larger than 1 MeV, is approximately the same as for Fe and Pb (see also Fig. 4), and low-energy  $\gamma$ -quanta are absorbed much better in Pb.

Note that the shape of the spectral distributions of photons after passing through the 15 and 25 cm thick shields made of Fe remains practically unchanged – only the number of transmitted photons changes. A similar situation occurs when photons pass through Pb shields with the thicknesses  $t_{eq}^{Pb} = 15$  and 25 cm.

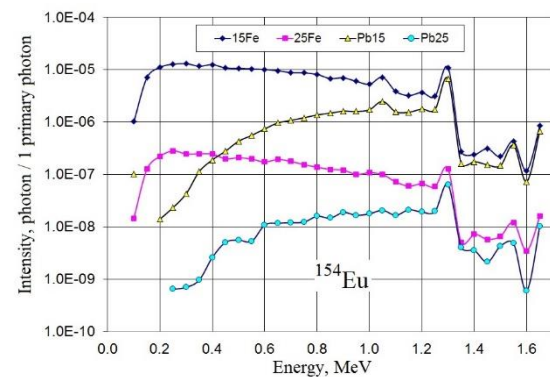


Fig. 6. The transformation of the spectrum of primary photons from the  $^{154}\text{Eu}$  isotope after passing through various shields

It is obvious that the radiation shielding properties of the combined shield depends on the placement order of the Fe and Pb layers due to the difference in the energy spectrum during the passage of  $\gamma$ -quanta through layers of the same mass thickness. A two-layer combined shield equivalent to iron thickness of 30 cm (mass thickness 235.8 g/cm<sup>2</sup>) is considered, in which the weight of iron and lead is the same, i.e. the thickness of the Fe layer is 15 cm, and the thickness of the Pb layer is equivalent to 15 cm of iron, which is 10.4 cm of lead. Two cases of the placement order of such shields are considered. In the first case, the first layer is of iron, and the second layer is of lead. And in the second case, the first layer is of lead, and the second layer is of iron. Table 3 shows the dose rate ratios  $D_{mat}(30)/D_{Fe}(30)$  produced by  $\gamma$ -quanta from  $^{60}\text{Co}$ ,  $^{154}\text{Eu}$ ,  $^{134}\text{Cs}$  isotopes behind shields with a thickness equivalent to 30 cm of iron. The dose ratios



$D_{mat(30)}/D_{Fe(30)}$  produced by neutrons from the  $^{244}\text{Cm}$  isotope, the main source of SNF neutrons, are also given.

Table 3

Dose rate ratios  $D_{mat(30)}/D_{Fe(30)}$  produced by  $\gamma$ -quanta and neutrons behind shields with a thickness equivalent to 30 cm of iron

No	Shielding material, equivalent thickness, cm	$D_{mat(30)}/D_{Fe(30)}$ , %			
		$^{60}\text{Co}$	$^{154}\text{Eu}$	$^{134}\text{Cs}$	$^{244}\text{Cm}$
1	Pb, equi 30 cm	13.1	13.0	7.9	169
2	Fe 15 cm + Pb equi 15 cm	23.2	22.9	12.8	114
3	Pb equi 15 cm + Fe 15 cm	48.5	47.4	30.0	125

It follows from the data given in Table 3 that lead is the most effective gamma shield; the maximum dose rate behind Pb shield is 13.1% of the dose rate behind Fe shield. The dose rate reduction is more than twice higher in the case of the combined shield in the first case, when the first layer is of Fe, than in the second case, when the first layer is of Pb. The shield of Fe is proved to be the most effective shield against neutrons. The dose rate produced by neutrons behind the Pb shield, which is equivalent to 30 cm Fe thick, is  $\sim 1.7$  times higher than behind the Fe shield. Behind the combined shield made of Fe and Pb, if the first layer is Fe, the dose rate is  $\sim 10\%$  smaller than for the shield with the first Pb layer.

The spectra of  $\gamma$ -quanta from the  $^{154}\text{Eu}$  isotope that passed through the shields of four different composition are shown in Fig. 7. These compositions are as follows. First one is 30 cm thick Fe shield. Second one is Pb shield with a thickness equivalent to 30 cm of Fe. Two other compositions are combined shields with different order of Pb and Fe.

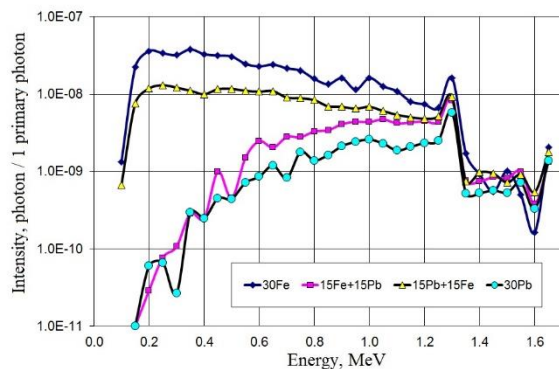


Fig. 7. Spectra of  $\gamma$ -quanta from  $^{154}\text{Eu}$  isotope that passed through the shield of Fe 30 cm thick, the shield of Pb and the combined shields made of Fe and Pb with 30 cm Fe equivalent thickness

The neutron spectra behind the same shields are shown in Fig. 8. Note that the spectra of neutrons passed through the combined shielding (Pb equi 15 cm + Fe 15 cm) are very close to the spectra of neutrons passed through 30 cm Pb and therefore are not shown in Fig. 8.

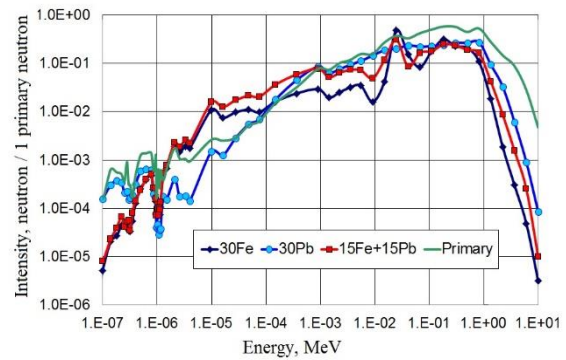


Fig. 8. Spectra of neutrons that passed through the shield of Fe 30 cm thick, the shield of Pb and the combined shield made of Fe and Pb with 30 cm Fe equivalent thickness

Table 3 shows the dose rate ratios produced by  $\gamma$ -quanta and neutrons behind combined shields, in which the mass thickness of the layers of lead and iron are the same, i.e. the ratio  $t_{Fe} \rho_{Fe}/(t_{Pb} \rho_{Pb}) = K_{mass} = 1$ . For NAC-STC TC  $K_{mass} = 0.77$ , and for TC HI-STAR190UA  $K_{mass} = 0.71$ , i.e. the weight of lead exceeds that of iron in the radiation shields of these TCs. The attenuations of  $\gamma$ -quanta by two-layer combined shields with a thickness equivalent to 30 cm Fe, in which  $K_{mass} = 0.8$  and  $0.6$ , are calculated. For example, it is shown for  $^{154}\text{Eu}$ , that the dose rate ratio  $D_{mat(30, K_{mass})}/D_{Fe(30)} = 21.6\%$  and  $19.9\%$  for combined shields where  $K_{mass} = 0.8$  and  $0.6$ , respectively, compared to  $D_{mat(30, 1)}/D_{Fe(30)} = 22.9\%$ . For the existing TC HI-STAR190UA, which are planned to be used for the transportation of SNF from Ukrainian NPPs to the Central Storage Facility (CSFSF), the radiation shielding characteristics of the TC are calculated. The model of the TC HI-STAR190UA is shown in Fig. 9. The disk shield model that simulates the HI-STAR190UA radiation shielding in the radial direction is demonstrated in Fig. 10.

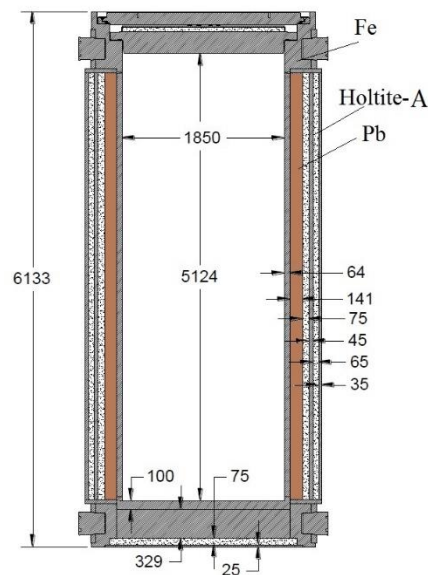


Fig. 9. Model of the HI-STAR190UA transport cask

Simulation of  $\gamma$ -quanta from the  $^{60}\text{Co}$  passage through the shield carried out in PHITS proves significant change in the photon flux. The passage of neutrons is simulated in the cylindrical model of the TC. The case named VAR is considered. It is described in Table 4. The thicknesses of the Fe layers are changed via the transferring the most of Fe to layer No. 1 and reducing the thicknesses of the layers No. 2 and 3. The thickness of the Pb layer, as well as the thickness of the Holite-A neutron shielding layers are fixed. Therefore the entire weight of the TC does not change.

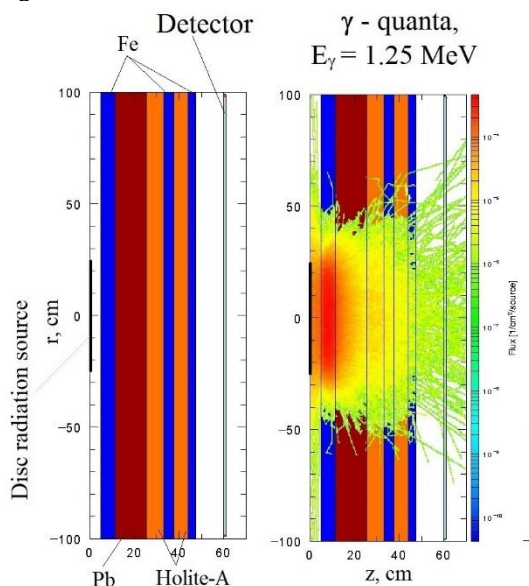


Fig. 10. The disk shield model

Table 4  
Thicknesses of the shield layers in the radial direction for TC HI-STAR190 UA and the case VAR

N layer	Layer material	Layer thickness, cm	
		190UA	VAR
1	Fe	6.4	<b>13.4</b>
2	Pb	14.1	14.1
3	Holite-A	7.5	7.5
4	Fe	4.5	<b>0.5</b>
5	Holite-A	6.5	6.5
6	Fe	3.5	<b>0.5</b>

Table 5 shows the calculated dose rate ratios produced by  $\gamma$ -quanta from  $^{154}\text{Eu}$ ,  $^{60}\text{Co}$  isotopes and by neutrons from  $^{244}\text{Cm}$  isotope after passing the HI-STAR 190UA shield ( $D_{\text{HI-190UA}}$ ) and after case VAR shield ( $D_{\text{VAR}}$ ).

Table 5  
Dose rate ratios produced by  $\gamma$ -quanta and neutrons after passing the HI-STAR190UA shield and the case VAR shield

	Isotope	$D_{\text{VAR}}/D_{\text{HI-190UA}}, \%$
1	$^{154}\text{Eu} - \gamma$	52
2	$^{60}\text{Co} - \gamma$	73
3	$^{244}\text{Cm}$ , neutrons	87

The performed calculations show that the redistribution of iron by changing the thickness of the

layers makes it possible to significantly increase the gamma shield efficiency and improve neutron shielding.

## CONCLUSIONS

Models of a radiation source of  $\gamma$ -quanta in the form of a cylinder surrounded by a cylindrical shield and a disk with a layered shield are developed for simulating the shielding of TCs for SNF transportation by railway. The Monte Carlo method is used to study the characteristics of  $\gamma$ -quanta from long-lived SNF isotopes after passage through shields of different thicknesses made of Fe and Pb. For the  $^{154}\text{Eu}$  and  $^{60}\text{Co}$  isotopes, the effectiveness of Pb shields is shown to increase with the thickness of the shields. For the  $^{134}\text{Cs}$  and  $^{137\text{m}}\text{Ba}$  ( $^{137}\text{Cs}$ ) isotopes, the shielding efficiency of Pb practically does not change with increasing the lead thickness. The influence of the order of placement of Fe and Pb layers in a combined two-layer radiation shield is investigated. The two-layer shields made of Fe and Pb of the same mass thickness are considered. Their entire thickness is equivalent to the iron thickness of 30 cm. Namely, the thickness of Fe layer is 15 cm, and that of Pb is 10.4 cm (the latter is equivalent to 15 cm of Fe). The efficiency of combined shield is shown to be more than twice higher in the case, if Fe is placed in the first layer and Pb – in the second layer, than if Pb is placed in the first layer and Fe – in the second layer. This is explained as follows. High-energy  $\gamma$ -quanta are transformed into low-energy  $\gamma$ -quanta during passage through the first Fe layer. The low-energy  $\gamma$ -quanta are effectively absorbed by the second Pb layer. The efficiency of  $\gamma$ -quanta absorption is shown to increase with an increase in the proportion (mass) of lead at a fixed weight of the combined shield. The transport of SNF neutrons emitted by the  $^{244}\text{Cm}$  isotope through combined Fe and Pb shields is studied as well. The maximum attenuation of the neutron flux is shown to be provided by the shields made of Fe, and the minimum – by the shields made of Pb. The efficiency of two-layer shield, in which Fe is placed in the first layer and Pb – in the second one, is shown to be by  $\sim 10\%$  higher than that of the combined layer, in which the first layer is made of Pb and the second layer – of Fe. Influence of both the thickness of the Fe layer and relocation of the iron to the first layer with fixed weight of both Fe and Pb on the neutron shielding of TCs HI-STAR190UA is studied. The proposed design of the layer placement order in the shield is shown to provide significant increase of the efficiency of the  $\gamma$ -quanta attenuation. Thus, to increase the efficiency of  $\gamma$ -quanta attenuation for a fuel cell with a combined shield made of Fe and Pb the first layer of radiation shield around the canister with SNF should be produced of iron of the maximum possible thickness.

## REFERENCES

1. *A Historical Review of the Safe Transport of Spent Nuclear Fuel*, FCRD-NFST-2016-000474 (Rev. 1), ORNL, Oak Ridge, 2016, 88 p.
2. *Managing Aging Effects on Dry Cask Storage Systems for Extended Long-Term Storage and Transportation of Used Fuel* – Rev. 2, Argonne National Laboratory, September 30, 2014 FCRD-UFD-2014-000476, ANL-13/15.

3. O.V. Grigorash, O.M. Dibach, S.M. Kondratiev, et al. Nutrition of nuclear and radiation safety of the centralized collection of the nuclear fuel fire of the NPP of Ukraine // *Nuclear and radiation safety*. 2017, v. 3(75), p. 3-10.
4. S. Alyokhina. Thermal state of ventilated storage container with spent nuclear fuel under normal operation // *International Journal of Nuclear Energy Science and Technology*. 2019, v. 13(4), p. 381-398; doi:10.1504/IJNEST.2019.106056
5. S. Alyokhina, A. Kostikov, S. Kruhlov. Safety issues of the dry storage of the spent nuclear fuel // *Problems of Atomic Science and Technology*. 2017, N 2(108), p. 70-74.
6. Y. Iwamoto, T. Sato, S. Hashimoto, et al. Benchmark study of the recent version of the phits code // *J. Nucl. Sci. Technol.* 2017, v. 54(5), p. 617-635; <https://doi.org/10.1080/00223131.2017.1297742>.
7. I.I. Zalubovsky, S.A. Pismenetskiy, V.G. Rudychev, et al. Protective structures for storing spent nuclear fuel from the Zaporozhye NPP // *Atomic Energy*. 2012, v. 112(4), p. 261-268.
8. Guang Hu, Huasi Hu, Quanzhan Yang, Bo Yu, Weiqiang Sun. Study on the design and experimental verification of multilayer radiation shield against mixed neutrons and g-rays // *Nuclear Engineering and Technology*. 2020, v. 52, p. 178-184.
9. V.G. Rudychev, N.A. Azarenkov, I.O. Girka, Ye.V. Rudychev. The efficiency of radiation shielding made of materials with high atomic number and low mass density // *Problems of Atomic Science and Technology. Series "Nucl. Phys. Invest."*. 2021, N 2(132), p.74-79.
10. P.M. Rinard, G.E. Bosler, J.R. Phillips. *Calculated Neutron Source Spectra from Selected Irradiated PWR. Fuel Assemblies*, Los Alamos National Laboratory, USA, 1981, LA-9125-MS.
11. Muhammad Arif Sazali et al. A review on multilayer radiation shielding 2019 IOP // *Conf. Ser.: Mater. Sci. Eng.* 555 012008.

Article received 28.06.2022

## **ЕФЕКТИВНІСТЬ КОМБІНОВАНОГО РАДІАЦІЙНОГО ЗАХИСТУ З Fe ТА Pb ТРАНСПОРТНИХ КОНТЕЙНЕРІВ ДЛЯ ПЕРЕВЕЗЕННЯ ВЯП**

***В.Г. Рудичев, М.О. Азаренков, І.О. Гірка, Є.В. Рудичев***

Досліджено можливість підвищення ефективності комбінованих захистів з Fe та Pb транспортних контейнерів (ТК) для перевезення ВЯП залізницею. Розроблено моделі транспорту  $\gamma$ -квантів ВЯП, що дозволяють визначити методом Монте-Карло потужності доз за захистами великої товщини. Показано, що для шарів однакової масової товщини: Fe = 15 см, Pb = 10.4 см еквівалентним 15 см заліза, розміщення в першому шарі Fe, а у другому – Pb послаблює потік квантів більш ніж удвічі. Досліджено ослаблення нейтронів ВЯП захистами з Fe та Pb. При перенесенні більшої частини заліза в перший шар без зміни ваги як Fe, так і Pb, в ТК HI-STAR190UA потік квантів ВЯП зменшується в ~ 1,5 рази.